Supplementary Material for

Geochronological reconstruction of glacial evolution in the Ésera valley (Central Pyrenees) during the last deglaciation

Ixeia Vidaller[1], Toshiyuki Fujioka[2], ASTER Team[3,*], Juan Ignacio López-Moreno[1], Ana Moreno[1]
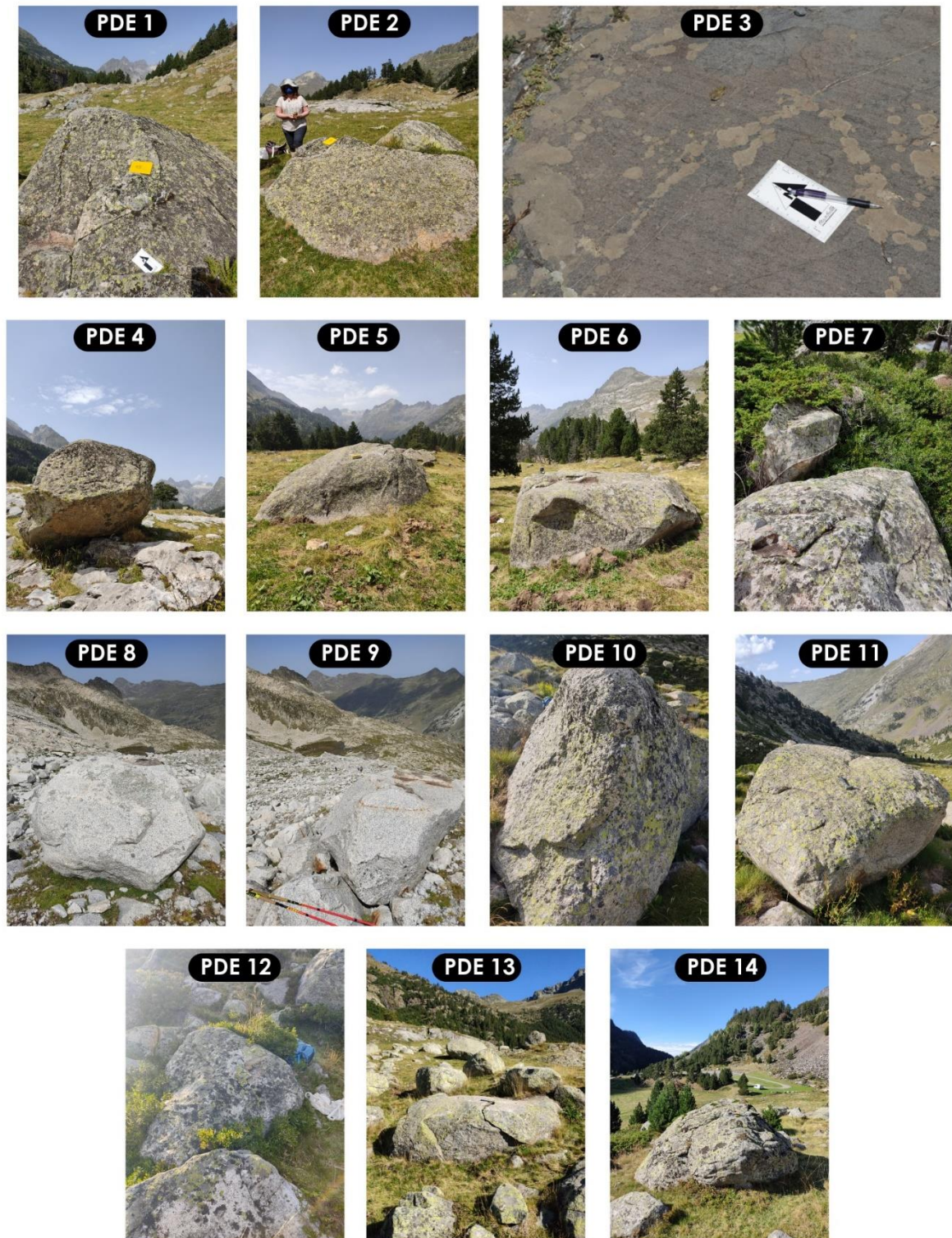
[1] Instituto Pirenaico de Ecología, Consejo Superior de Investigaciones Científicas (IPE-CSIC), Zaragoza, Spain
[2] Centro Nacional de Investigación sobre la Evolución Humana (CENIEH), Burgos, Spain
[3] CNRS, Aix Marseille Univ, IRD, INRAE, CEREGE, Aix-en-Provence, France
[3] Aster Team: G. Aumaître, K. Keddadouche, F. Zaïdi

Correspondence to: Ixeia Vidaller (ixeia@ipe.csic.es)

Figure S1: Photographs of the samples taken in the Ésera valley and Maladeta massif. PDE-1 and -2 corresponds with the samples located in the threshold of Pllan d'Están basin; PDE-3 and -4 are located in a threshold in the middle of Pllan d'Están basin; PDE-5, -6 and -12 correspond with a till between Pllan d'Están and Aiguallut ponor; PDE-7 is located near to Renclusa hut; PDE-8 and -9 are boulders of the Aneto LIA moraine; PDE-10 and -11 corresponds to a moraine between Aiguallut ponor and Barrancs lake; and PDE-13 and -14 are granitic blocks of the moraine of Llanos del Hospital.
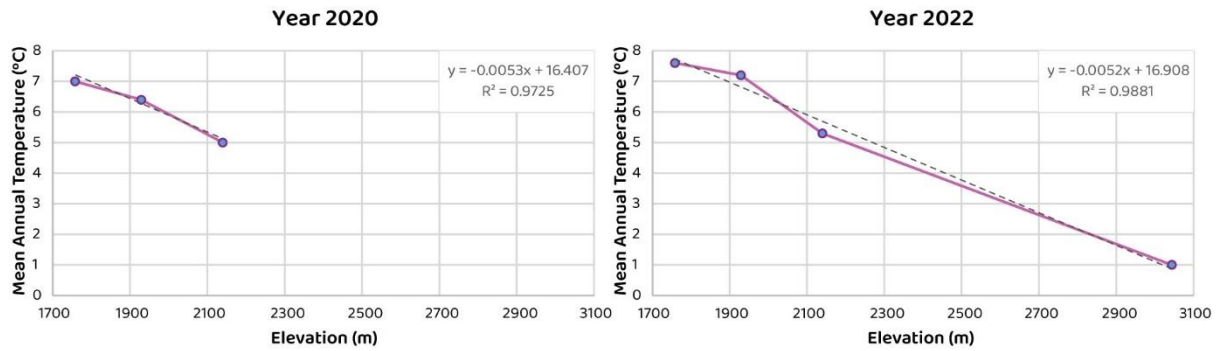
Figure S2: Altitudinal gradient of temperature for the years 2022 and 2020 based on the data of some weather station of the headwaters of Ésera valley.

ID	Latitude (ºN)	Longitude (ºE)	Elevation (m)	Thickness (cm)	Topographic shielding	Boulder height above ground (cm)	Snow shielding [a]	Snow shielding [a, b]
PDE1	42.6820	0.6337	1848	2.48	0.9318	160	0.9954	0.8622
PDE2	42.6816	0.6344	1849	2.13	0.9605	50	0.9178	0.8622
PDE3	42.6810	0.6452	1880	3.04	0.9845	-	0.8622	-
PDE4	42.6807	0.6433	1854	2.11	0.9190	200	1.0000	-
PDE5	42.6766	0.6539	1933	1.59	0.9684	120	0.9730	-
PDE6	42.6768	0.6530	1937	1.37	0.9800	125	0.9758	-
PDE7	42.6723	0.6522	2039	3.87	0.9670	160	0.9954	-
PDE8	42.6487	0.6579	2660	4.35	0.9909	126	0.9764	-
PDE9	42.6496	0.6585	2634	1.87	0.9910	120	0.9730	-
PDE10	42.6555	0.6661	2189	2.04	0.9393	140	0.9844	-
PDE11	42.6555	0.6661	2195	1.72	0.9660	180	0.9999	-
PDE12	42.6726	0.6617	1995	4.68	0.9597	80	0.9448	-
PDE13	42.6831	0.6057	1755	3.44	0.8113	70	0.9367	-
PDE14	42.6830	0.6058	1744	4.42	0.8523	120	0.9730	-

Table S1: Sample and field data. All samples were collected from granitic erratic boulder surfaces except PDE3, which was collected from a glacially-polished quartzite bedrock surface. Density is assumed to be 2.65 g/cm³ for all samples. (a) Calculated using a formula (Eq. 3.76) in Gosse and Phillips (2001) with average monthly snow accumulation during 20087-2023 (AEMET database). (b) Calculated without considering boulder height above ground (see main text for details).

Field ID	Quartz mass (g)	^{9}Be spike (mg)	^{27}Al (ug/g(Qz))	^{10}Be/^{9}Be (10^{-13}) [a]	Err	^{26}Al/^{27}Al (10^{-13}) [b]	Err	^{10}Be [c] (10^5 atoms/g(Qz))	Err [e]	^{26}Al [d] (10^5 atoms/g(Qz))	Err [e]	^{26}Al/^{10}Be	Err
PDE1	12.04	0.2686	249.8	1.258	0.044	-	-	1.830	0.068	-	-	-	-
PDE2	12.08	0.2666	295.3	1.265	0.040	-	-	1.820	0.063	-	-	-	-
PDE3	3.01	0.2517	2033.8	0.367	0.027	0.339	0.065	1.906	0.153	15.2	3.0	8.0	1.7
PDE4	12.04	0.2713	252.8	1.500	0.049	-	-	2.213	0.077	-	-	-	-
PDE5	12.01	0.2688	940.3	1.505	0.051	-	-	2.206	0.082	-	-	-	-
PDE6	12.01	0.2682	254.5	1.462	0.047	-	-	2.136	0.074	-	-	-	-
PDE7	12.17	0.2679	328.2	1.712	0.055	-	-	2.474	0.08.5	-	-	-	-
PDE8	30.17	0.2225	257.0	0.314	0.023	-	-	0.140	0.012	-	-	-	-
PDE9	30.07	0.2229	223.6	0.293	0.033	-	-	0.130	0.016	-	-	-	-
PDE10	12.04	0.2677	258.4	1.481	0.068	-	-	2.155	0.138	-	-	-	-
PDE11	12.05	0.2682	276.1	1.516	0.051	-	-	2.209	0.080	-	-	-	-
PDE12	12.08	0.2688	233.1	1.513	0.051	-	-	2.204	0.071	-	-	-	-
PDE13	12.05	0.2684	227.2	1.344	0.044	-	-	1.955	0.069	-	-	-	-
PDE14	12.05	0.2686	136.1	1.405	0.052	-	-	2.048	0.081	-	-	-	-

Table S2: Laboratory data. All samples were processed to beryllium hydroxides in Cosmogenic Nuclide Dating Laboratory at CENIEH and then calcined to oxides in ASTER. Uncertainties are in one sigma. (a) Measured in ASTER against the standard STD-11 with the nominal ^{10}Be/^{9}Be ratio of 1.191 ± 0.013 x 10^{-11}, which was calibrated against the standard NIST SRM4325 with the nominal ratio of 2.79 ± 0.03 x 10^{-11} (Braucher et al., 2015). (b) Measured in ASTER against the standard SM-Al-11 with the nominal ^{26}Al/^{27}Al ratio of 7.401 ± 0.064 x 10^{-12} (Arnold et al., 2010; Merchel and Bremser, 2004). (c) Corrected for procedural blanks with the ^{10}Be/^{9}Be ratios of 2.6-4.0 x 10^{-15}. (d) Corrected for procedural blanks with the ^{26}Al/^{27}Al ratios of 1.6-5.5 x 10^{-15}. (e) Calculated from AMS uncertainties (counting statistics, standard reproducibility, error in the standard nominal ratio, blank correction) and, for ^{10}Be, 1% error in ^{9}Be spike concentration, and, for ^{26}Al, 3% error in ICP-OES Al measurements, in quadrature.

Field ID	With no snow shielding [a]						With snow shielding [b]						With snow shielding ignoring boulder heights [c]					
	At 0 mm/ka (Minimum ages)	Int. err	Ext. err	At 3 mm/ka	Int. err	Ext. err	At 0 mm/ka	Int. err	Ext. err	At 3 mm/ka	Int. err	Ext. err	At 0 mm/ka	Int. err	Ext. err	At 3 mm/ka	Int. err	Ext. err
PDE1	11.68	0.44	0.82	11.97	0.46	0.86	11.72	0.44	0.82	12.02	0.46	0.87	13.24	0.49	0.93	**13.68**	**0.53**	**0.99**
PDE2	11.28	0.39	0.77	11.58	0.41	0.82	12.14	0.42	0.83	12.47	0.45	0.88	12.80	0.45	0.88	**13.17**	**0.47**	**0.93**
PDE3	11.34	0.92	1.14	11.63	0.97	1.20	12.86	1.04	1.29	**13.24**	**1.11**	**1.37**	-	-	-	-	-	-
PDE4	13.87	0.49	0.95	14.34	0.52	1.02	13.87	0.49	0.95	**14.34**	**0.52**	**1.02**	-	-	-	-	-	-
PDE5	12.47	0.45	0.87	12.82	0.48	0.92	12.76	0.47	0.89	**13.12**	**0.49**	**0.94**	-	-	-	-	-	-
PDE6	11.96	0.42	0.82	12.27	0.44	0.87	12.20	0.42	0.84	**12.54**	**0.45**	**0.89**	-	-	-	-	-	-
PDE7	13.07	0.45	0.90	13.49	0.48	0.96	13.12	0.46	0.90	**13.55**	**0.49**	**0.96**	-	-	-	-	-	-
PDE8	0.420	0.036	0.044	0.420	0.036	0.044	0.429	0.037	0.045	**0.429**	**0.037**	**0.045**	-	-	-	-	-	-
PDE9	0.390	0.050	0.055	0.390	0.050	0.055	0.400	0.051	0.056	**0.401**	**0.051**	**0.057**	-	-	-	-	-	-
PDE10	10.65	0.51	0.81	10.91	0.54	0.86	10.80	0.52	0.83	**11.07**	**0.55**	**0.87**	-	-	-	-	-	-
PDE11	10.56	0.38	0.73	10.81	0.40	0.77	10.56	0.39	0.73	**10.81**	**0.40**	**0.77**	-	-	-	-	-	-
PDE12	12.32	0.44	0.85	12.66	0.47	0.91	12.93	0.47	0.90	**13.33**	**0.50**	**0.96**	-	-	-	-	-	-
PDE13	15.03	0.53	1.04	15.60	0.58	1.12	15.99	0.57	1.10	**16.64**	**0.62**	**1.20**	-	-	-	-	-	-
PDE14	15.23	0.61	1.09	15.82	0.65	1.17	15.63	0.62	1.11	**16.26**	**0.67**	**1.21**	-	-	-	-	-	-

Table S3: [10]Be exposure ages (ka). All ages were calculated using CRONUS-Earth online calculator (https://hess.ess.washington.edu/, Balco et al., 2008) with wrapper version 3.0.2. Here, ages using LSDn scaling (Lifton et al., 2014) are shown. Two cases of erosion rates were assumed, i.e., 0 and 3 mm/ka. Uncertainties are in one sigma. "Int."(internal) errors only include analytical errors and "Ext." (external) errors also include systematic errors (e.g., half-life, production rates). When compared to other geochronological data, external errors must be considered. Values in bold denote 'Best ages' shown in Table 1 in the main text. (a) Calculated without snow shielding. (b) Calculated with snow shielding (see Supplementary Table S1). (c) Calculated with snow shielding ignoring boulder heights for the samples PDE-1 and PDE-2 (see Supplementary Table S1).

References

Arnold, M., Merchel, S., Bourlès, D., Braucher, R., Benedetti, L., Finkel, R., Aumaître, G., Gottdang, A., and Klein, M.: The French accelerator mass spectrometry facility ASTER: Improved performance and developments, Nucl. Instruments Methods Phys. Res. Sect. B-beam Interact. With

20 Mater. Atoms - NUCL INSTRUM METH PHYS RES B, 268, 1954–1959, https://doi.org/10.1016/j.nimb.2010.02.107, 2010.

Balco, G., Stone, J. O., Lifton, N. A., and Dunai, T. J.: A complete and easily accessible means of calculating surface exposure ages or erosion rates from 10Be and 26Al measurements, Quat. Geochronol., 3, 174–195, https://doi.org/https://doi.org/10.1016/j.quageo.2007.12.001, 2008.

Braucher, R., Guillou, V., Bourlès, D. L., Arnold, M., Aumaître, G., Keddadouche, K., and Nottoli, E.: Preparation of ASTER in-house 10Be/9Be standard solutions, Nucl. Instruments Methods Phys. Res. Sect. B Beam Interact. with Mater. Atoms, 361, 335–340,

25 https://doi.org/https://doi.org/10.1016/j.nimb.2015.06.012, 2015.

Gosse, J. C. and Phillips, F. M.: Terrestrial in situ cosmogenic nuclides: theory and application, Quat. Sci. Rev., 20, 1475–1560, https://doi.org/https://doi.org/10.1016/S0277-3791(00)00171-2, 2001.

Lifton, N., Sato, T., and Dunai, T.: Scaling in situ cosmogenic nuclide production rates using analytical approximations to atmospheric cosmic-ray fluxes, Earth Planet. Sci. Lett., 386, 149–160, https://doi.org/10.1016/j.epsl.2013.10.052, 2014.

30 Merchel, S. and Bremser, W.: First international 26Al interlaboratory comparison – Part I, Nucl. Instruments Methods Phys. Res. Sect. B Beam Interact. with Mater. Atoms, 223–224, 393–400, https://doi.org/https://doi.org/10.1016/j.nimb.2004.04.076, 2004.